Separation Science and Technology
Publication details, including instructions for authors and subscription information:
http://www.informaworld.com/smpp/title~content=t713708471

Field-Flow Fractionation

J. Calvin Giddings[a]
[a] DEPARTMENT OF CHEMISTRY, UNIVERSITY OF UTAH SALT LAKE CITY, UTAH

To cite this Article Giddings, J. Calvin(1984) 'Field-Flow Fractionation', Separation Science and Technology, 19: 11, 831 — 847
To link to this Article: DOI: 10.1080/01496398408068596
URL: http://dx.doi.org/10.1080/01496398408068596

SEPARATION SCIENCE AND TECHNOLOGY, **19**(11 & 12), pp. 831-847, 1984-85

Field-Flow Fractionation

J. CALVIN GIDDINGS

DEPARTMENT OF CHEMISTRY
UNIVERSITY OF UTAH
SALT LAKE CITY, UTAH 84112

INTRODUCTION

Field-flow fractionation (FFF) is a separation method first described in 1966 (*1*). FFF is an elution technique, like chromatography, and the experimental sequence of pump, column, detector, and fraction collector is much like that used in chromatographic operations (*2–4*). However, FFF appears to be unique in its ability to separate an extremely broad range of molecules, macromolecules, supramacromolecular structures, colloidal particles, and larger particles at a high level of resolution. In dealing with these complex and often refractory materials, FFF has a number of unique advantages (*5*). Along with its intrinsically high resolving power, FFF is a versatile technique in which experimental conditions can be varied widely to optimize the range, speed, and power of the separation. FFF is also unusual in that the characteristics of the separation can be calculated rather exactly in terms of well-defined physicochemical parameters such as molecular weight, size, charge, etc. The equations used for this purpose can be inverted to yield molecular weight and other important parameters for the components of complex mixtures (*3–6*).

FFF developed slowly following its introduction in 1966. Most of the work reported since that time has been carried out in our laboratory at the University of Utah. In recent years a large number of groups has begun to work on FFF. Some excellent work in the development of one of the subtechniques of FFF, sedimentation FFF, has been done by Kirkland and Yau of the DuPont Company (*7, 8*); this appears to be a precursor to commercial instrumentation. We note that the development of FFF was

 0149-6395/84/1911-0831$3.50/0

initially slowed by the rather demanding requirements of high resolution FFF instrumentation and by the intrinsic difficulties of working with the macromolecular/colloidal materials involved.

The enormous breadth of applicability of FFF is one of its most exciting characteristics. The method appears applicable to virtually any type of soluble/suspendable macromolecular or colloidal material. The solvent/suspending medium can be aqueous or organic. The particles may be charged, uncharged, random coil, or globular; they may originate as a consequence of industrial, biological, environmental, or geological activities. The range of particle mass to which FFF has been found applicable is very large, extending from a molecular weight of 10^3 to an effective molecular weight of 10^{18}, the latter corresponding to 100 μm diameter. The mass range covered is therefore approximately 10^{15}; this range will certainly be extended in the future. There are no apparent gaps in this range that cannot be handled by some form of FFF.

FFF separations are carried out in a thin, ribbonlike flow channel. A field or gradient is applied across the thin dimension of the ribbonlike space as shown in Fig. 1. The field must be of a type that interacts with the soluble or suspendible species contained in the carrier fluid within the channel. The interaction forces the particles toward one wall (termed the accumulation wall) of the channel. Different levels of interaction for different species lead to the formation of layers or "clouds" of different thicknesses near the wall. After the layers have established their steady-state configuration, in which displacement toward the wall is balanced by diffusion away from the wall, flow is initiated in the channel. The resulting parabolic flow profile carries the particle clouds downstream. However, species that form the most compact layers against the wall are displaced more slowly than species forming diffuse layers because the velocity of parabolic flow is slowest near the wall. Therefore, different species forming different layer thicknesses as a

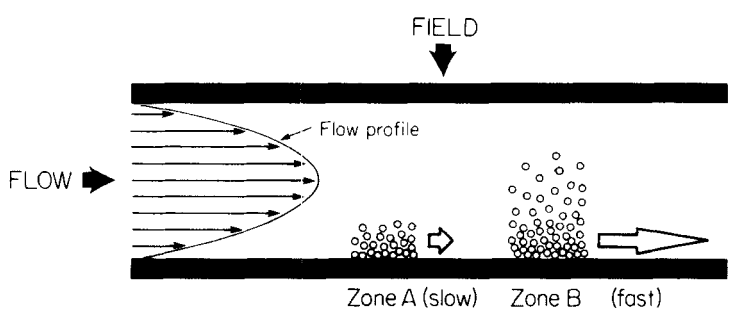

FIG. 1. Edge view of FFF channel showing the perpendicular orientation of field and flow vectors and the separation of Zones A and B.

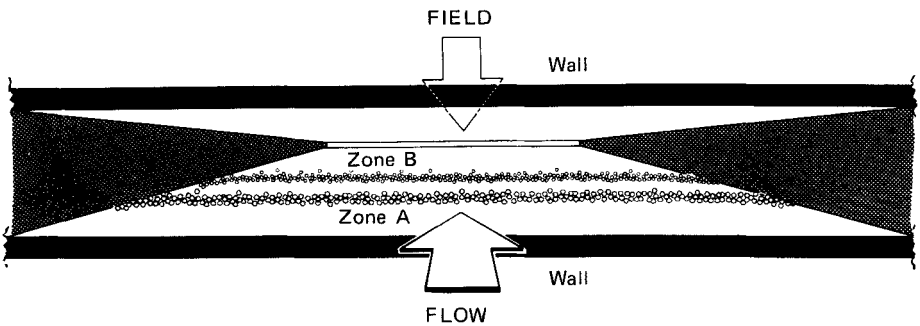

FIG. 2. End view of FFF channel in which Zones A and B are being separated.

consequence of unequal interactions with the field are displaced differentially and form separated zones within the channel. This process is illustrated in Fig. 1, which is a schematic view looking into an FFF channel from the edge. This figure shows the zone corresponding to the less interactive and therefore more diffuse layer of Component B moving ahead of the zone for the more interactive Component A. An end view of the separation of Component B from Component A is shown in Fig. 2. Channel aspect (breadth/thickness) ratios may typically range from 40 to 200.

A number of different fields or gradients can be used to implement separation in FFF depending upon the particle characteristics one wishes to utilize as a basis of separation. For example, if we want to separate a particle mixture on the basis of different electrical charges, then an electrical field would be applied. This subtechnique of FFF is termed electrical FFF. If it were considered desirable to separate on the basis of mass differences, then the channel would be coiled inside a centrifuge, leading to the subtechnique of sedimentation FFF. The four prominent subtechniques are shown in Fig. 3. Along with the two mentioned above, we have thermal FFF, which is based on thermal diffusion along a steep temperature gradient dT/dx established across the FFF channel, and flow FFF, which is based on a slow crossflow of carrier fluid entering the channel by penetrating through semipermeable membrane walls. Other subtechniques discussed in the literature include concentration gradient FFF (*9*), magnetic FFF (*10*), and shear FFF (*11*). We are currently working on theoretical aspects of dielectrical FFF.

In addition to the variety of field types (subtechniques) applicable to FFF, the steady-state particle layer can be formed in several basic ways. In normal FFF, illustrated in Fig. 1, an exponential particle density profile is formed as a consequence of a balance between field-induced migration and particle

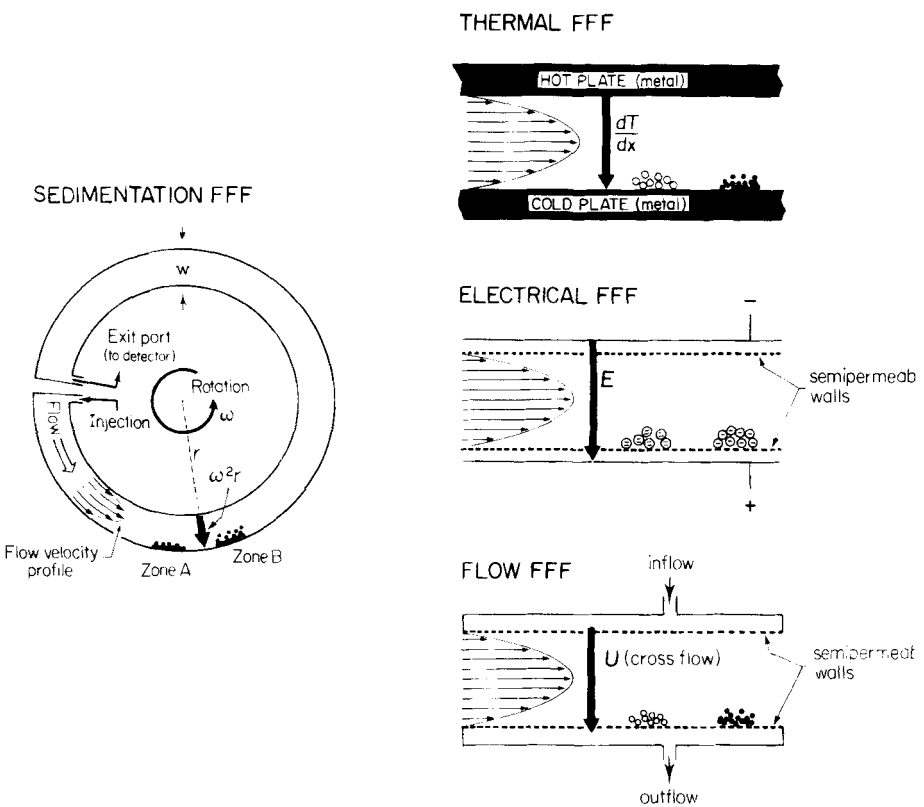

FIG. 3. Four prominent subtechniques of FFF.

diffusion. In steric FFF, by contrast, particles are forced into a thin uniform layer at or very close to the wall. In this case, diffusion is negligible; the protrusion of the particles into the flow stream is determined by their physical size (*12*). In hyperlayer FFF (yet to be implemented), the particles are forced into a thin layer removed from the wall (*13*). The freely suspended layers of hyperlayer FFF resemble the stationary zones of isoelectric focusing, but they are translated downstream by flow and can be separated even if they initially overlap. The three basic layer configurations mentioned above are summarized in Fig. 4.

The applicability of FFF to macromolecules and colloids is largely attributable to the fact that separation occurs within one phase, thus minimizing interactions with interfaces. In addition, the technique is rather gentle, lacking the extensional shear of chromatographic systems, an important advantage for fragile species.

The high resolving power and relatively high speed of FFF is due to the fact that thin, well-defined particle layers (in any one of the three categories mentioned above) can be formed in the channel space. The different layers (corresponding to the various species) occupying different mean positions are then differentially displaced by the highly nonuniform flow profile in the channel. The resulting separation is therefore highly selective (*14*).

The versatility of FFF stems from the fact that many parameters controlling the separation can be varied precisely over wide limits (5). Geometrical parameters such as channel thickness and length can be fixed at any desired level. More importantly, field strength can be varied continuously and almost instantly over a wide range of values to suit the problem at hand. Different field types have been found especially suitable for different classes of materials. Finally, the flow velocity, which directly controls resolution and speed, can be adjusted at any level that best accommodates experimental goals.

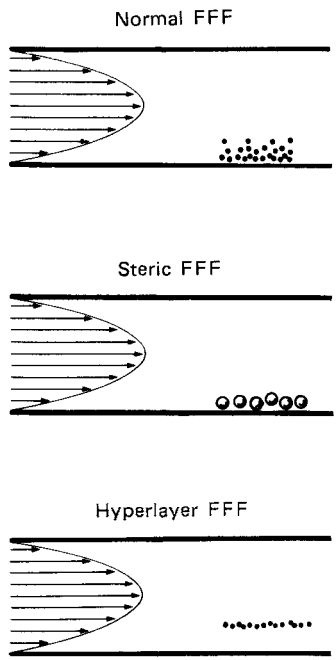

FIG. 4. Three basic configurations of steady-state layers in FFF.

THEORY

The theory of FFF has been extensively developed in the years since its inception (*15–21*). Below we will present only the most basic elements of theory necessary to understand the fundamentals and optimization of FFF systems.

We begin by assuming that steady-state conditions are established across the channel (*15*). For normal FFF this means that the rate of particle transport toward the accumulation wall caused by interaction with the applied field is exactly balanced by the transport away from the wall due to diffusion. Once this balance is established, theory shows that the particle distribution is exponential:

$$c = c_0 e^{-x/l} \tag{1}$$

where c is the concentration of particles at distance x from the accumulation wall, c_0 is the concentration at the wall, and l is a characteristic (mean) layer thickness given by

$$l = D/U \tag{2}$$

in which D is the particle diffusion coefficient and U is the particle drift velocity induced by the field.

Of great importance to the mathematical linkage of theory and experiment is the retention parameter λ, which is essentially a dimensionless form of l

$$\lambda = l/w = D/Uw \tag{3}$$

where w is the channel thickness. If we use the Stokes-Einstein equation for D,

$$D = kT/f \tag{4}$$

and the basic relationship between U and the force F acting on the particle,

$$U = F/f \tag{5}$$

then the expression for λ given by Eq. (3) becomes

$$\lambda = kT/Fw \tag{6}$$

where k is Boltzmann's constant, T is temperature, and f has been used to represent the friction coefficient. Equation (6) shows that λ is the dimensionless ratio of two energies: thermal energy kT and the energy expended in moving a particle across channel thickness w. Combining Eqs. (3) and (6), we find that mean layer thickness l is given by

$$l = kT/F \tag{7}$$

This equation shows that the l value pertaining to any particular species is inversely proportional to the force of interaction of that species with the applied field. Different interactive forces therefore lead to different layer thicknesses for different species.

The particle cloud described by Eqs. (1) through (7) is displaced downstream by the parabolic flow profile. The velocity within the parabolic flow profile is distributed according to the expression

$$v = 6\langle v\rangle \left[\frac{x}{w} - \left(\frac{x}{w} \right)^2 \right] \tag{8}$$

where $\langle v\rangle$ is the mean cross-sectional velocity. By averaging the above displacement velocity of the different laminar layers, weighted by the concentration in that layer as expressed by Eq. (1), we arrive at the mean displacement velocity for a given particle type

$$\mathscr{V} = R\langle v\rangle \tag{9}$$

where the retention ratio R is found to be related to λ by (*16*)

$$R = 6\lambda \left[\coth\frac{1}{2\lambda} - 2\lambda \right] \tag{10}$$

For highly interactive fields, λ is small and R reduces to the simple form

$$R = 6\lambda \tag{11}$$

The time required to sweep a void peak (consisting of molecules unaffected by the field) through the FFF channel is given simply by the ratio of channel length L to mean velocity $\langle v\rangle$:

$$t^\circ = L/\langle v\rangle \tag{12}$$

The transit (or retention) time t_r for a collection of particles interacting with the field and traveling at the velocity expressed by Eq. (9) is given by

$$t_r = L/\bar{V} = L/R\langle v \rangle \tag{13}$$

From the last two equations, the ratio of retention time to void peak time is

$$t_r/t^\circ = 1/R \tag{14}$$

which shows that t_r increases in inverse proportion to R. Since the volume of fluid required to sweep retained and void peaks through the channel is proportional to the respective transit times, we have a like ratio for retention volume to void volume:

$$V_r/V^\circ = 1/R \tag{15}$$

where the volume V° necessary to transport a void peak through the channel is essentially equal to the physical (void) volume of that channel.

If we substitute λ from Eq. (6) into the R expression of Eq. (10), and substitute the latter into Eq. (15), we end up with a precise relationship between retention volume V_r, which is measurable for any discrete species, and the interaction force F

$$V_r = \frac{FwV^\circ}{6kT\left[\coth\frac{Fw}{2kT} - \frac{2kT}{Fw}\right]} \tag{16}$$

When Fw is much greater than kT, Eq. (11) can be used in place of Eq. (10), yielding the simple relationship

$$V_r = \frac{FwV^\circ}{6kT} \tag{17}$$

This equation shows that the components emerging in the effluent of an FFF channel are distributed along the retention volume (and time) axis in proportion to the strength of their interaction with the applied field. In other words, eluted components are distributed in a linear relationship to force, i.e., they form a linear force spectrum. In sedimentation FFF, where force F is proportional to particle mass, the elution spectrum is therefore a linear mass spectrum of component particles.

When samples consist of particles having an extremely wide range of sizes, the elution spectra expressed by Eqs. (16) and (17) are inconvenient because the elution volume range is too great and the last particles to emerge spend excessively long times in the channel. In this case, various forms of programming can be used to increase the elution speed of the more retained components. The first such technique developed was field programming, in which the field strength is gradually reduced in the course of the run so that the highly retained components emerge earlier (*22*). Kirkland and Yau have developed exponential forms of field programming such that the particle size distribution is logarithmic (*8*). One can also use flow programming, in which mean flow velocity $\langle v \rangle$ increases in the course of the run (*23*). Flow programming has some theoretical advantages over field programming, but may lead to sample detection problems because of the variable flow rate.

For either field or flow programming, the basic descriptive equation is (*22*)

$$L = \int_0^{t_r} R\langle v \rangle dt \tag{18}$$

which is an integral equation relating the particle mass or other critical property (implicit in R) to retention time t_r. For field programming, R is varied as a function of time by virtue of variations in field strength; for flow programming, $\langle v \rangle$ is changed with time.

As is clear from the preceding discussion, separation takes place because of the different levels of interaction of different particles with the applied field. The level of interaction of a given particle with the field depends upon some specific particle parameter, such as charge or mass, depending upon whether the field is electrical, sedimentation, etc. The impact of the interaction force F on FFF retention is best evaluated by calculating λ from Eq. (6) for subsequent use in Eq. (10) or (11). Expressions for λ have been worked out over time for the various subtechniques; these expressions are summarized in Table 1. In the right-hand column we show various particle parameters that influence λ and thus affect retention. Since the mathematical equations for retention (such as Eq. 10) are quite rigorous, one can turn this calculation around and deduce various combinations of these parameters from the experimental retention data. The use of this process for the accurate characterization of colloidal particles has been discussed elsewhere (*6, 24, 25*).

The retention equations for steric FFF and hyperlayer FFF also appear in fairly simple mathematical form (*12, 13*). However, in the remainder of this article we will confine our attention to normal FFF as described by the preceding equations.

TABLE 1
Expressions for Retention Parameter λ[a]

Subtechnique	λ equation	Particle parameters controlling retention
All FFF	$\lambda = \frac{D}{Uw} = \frac{RT}{Fw}$	
Sedimentation FFF	$\lambda_s = \frac{D}{sGw} = \frac{RT}{GM(1-\rho/\rho_s)w}$	M, ρ_s, s, D
Flow FFF	$\lambda_F = \frac{DV^\circ}{V_c w^2} = \frac{RTV^\circ}{3\pi\eta N V_c w^2 d}$	D, d
Electrical FFF	$\lambda_E = \frac{D}{\mu E w}$	μ, D
Thermal FFF	$\lambda_T = \frac{D}{D_T w(dT/dx)} = \frac{T}{\alpha w(dT/dx)}$	D_T, α

[a] *General symbols:*
w = channel thickness
U = mean field-induced velocity
F = field-induced force/mole
R = gas constant
T = absolute temperature
G = gravitational acceleration
ρ = solvent density
V° = void volume of column
V_c = volumetric crossflow rate
N = Avogadro's number
η = viscosity of solvent
E = electrical field strength
Particle characteristics:
D = diffusion coefficient
M = molecular weight
d = Stokes diameter
μ = electrophoretic mobility
D_T = coefficient of thermal diffusion
α = thermal diffusion factor
ρ_s = density
s = sedimentation coefficient

TABLE 2
Maximum Values of Column Selectivity, S_{max}, for Various FFF Subtechniques and for Size Exclusion Chromatography (SEC)

Subtechnique	S_{max}
Thermal FFF	0.5–0.6
Flow FFF	0.5–0.55
Sedimentation FFF	1
SEC	0.05–0.22

We note that the intrinsic resolving power of a separation technique can be expressed in terms of selectivity S. If separation occurs by virtue of differences in mass (as in sedimentation FFF), then the appropriate selectivity is the mass selectivity expressed by (*26*)

$$S = \left| \frac{d \ln V_r}{d \ln M} \right| \tag{19}$$

In the high retention limit for which Eq. (17) is valid, S reaches its maximum value which is seen to be

$$S_{max} = \left| \frac{d \ln F}{d \ln M} \right| = \left| \frac{d \ln \lambda}{d \ln M} \right| \tag{20}$$

where the last expression is derived from Eq. (6). Values for S_{max} for the various FFF subtechniques and for size exclusion chromatography are shown in Table 2. This table shows that sedimentation FFF has the highest selectivity of the presently practiced techniques. However, it has been shown theoretically that shear FFF, if it can be experimentally implemented, may have an S_{max} value as large as 3 (*11*).

We turn our attention now to the broadening of component zones in FFF channels. Zone broadening, which profoundly affects resolution, is illustrated in Fig. 5. For pure components the broadened zone assumes the form of a Gaussian concentration profile (*15*, *27*). The width of the Gaussian can be expressed by its standard deviation σ, but a better index of peak broadening in FFF (and other chromatographic-like methods) is the plate height H, expressed as

$$H = \sigma^2 / L \tag{21}$$

In well-designed FFF channels operating under normal flow conditions with pure components, the plate height can be shown to have the form (*17*)

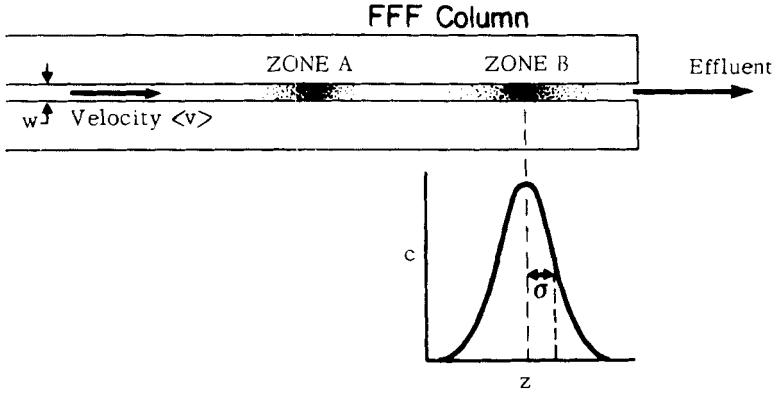

FIG. 5. Zone broadening in an FFF channel or column. The extent of zone broadening is measured by plate height H, expressed as σ^2/channel length.

$$H = \chi \frac{w^2\langle v \rangle}{D} \tag{22}$$

in which χ is a complicated function of λ. In the high retention limit, χ reduces to the simple expression

$$\chi = 24\lambda^3 \tag{23}$$

The last two equations show immediately why the high retention limit ($\lambda \ll 1$) is of practical interest. Clearly, as λ decreases, plate height and zone broadening decrease dramatically.

We note in passing that the steady-state approximation used to derive retention equations must be partially abandoned when considering zone broadening. This is because the differential flow profile forces a small departure from steady-state conditions. This departure, although not large numerically, is responsible for the bulk of zone broadening in FFF channels as expressed by Eq. (22).

APPLICATIONS

Field-flow fractionation has been applied to a wide variety of macromolecular and colloidal materials in the past decade. Sedimentation FFF is the subtechnique applied to the greatest number of materials up to this time. Sedimentation FFF, which Table 2 shows to have the highest level of selectivity of any of the common macromolecular/colloidal separation

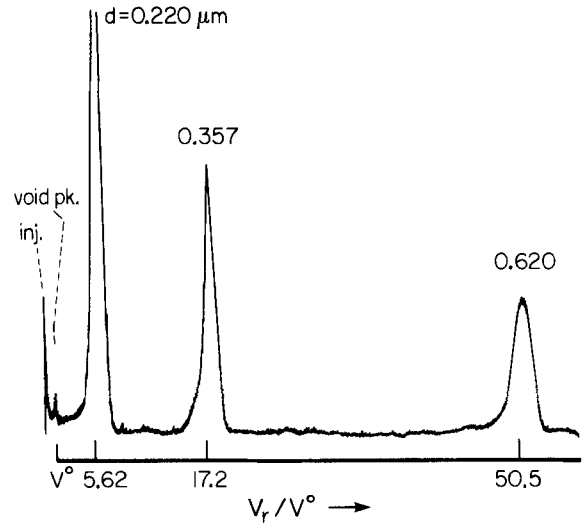

FIG. 6. Separation of polystyrene latex beads of different diameters by sedimentation FFF at 1850 rpm.

systems, is capable of resolving colloidal particles at exceedingly high resolution. Figure 6 illustrates this point by showing the separation of several polystyrene latex beads. Other species fractionated in our laboratory include PVC latices (*23*), several oil-in-water emulsions (*24*) including artificial blood (*28*), a number of virus particles (*29, 30*), waterborne colloids (*31*), liposomes (*32*), and albumin spheres (*33*). Kirkland and Yau at DuPont have also worked with a variety of materials in recent years (*34*).

Flow FFF is capable of handling materials of much lower molecular weight. Figure 7 shows the separation of various proteins by flow FFF (*35*). We have also fractionated small silica beads (*36*), viruses (*37*), latices (*38*), water-soluble polymers (*39*) and, more recently, lipophilic polymers (*40*). While flow FFF has not yet been as widely applied as sedimentation FFF, and while its selectivity is not as great, it has the advantage of being applicable to species of both low and high molecular weight. In fact, flow FFF can be considered to be the most universally applicable FFF method, in large part because the lateral driving force (flow) interacts by means of frictional drag with every conceivable molecular and particulate species. Flow FFF should eventually be applicable to any soluble or suspendable species for which a semipermeable membrane can be found.

We have applied thermal FFF to lipophilic polymers; the thermal diffusion effect appears to be too weak to work effectively in most aqueous solutions. Linear polystyrenes have been studied most extensively (*41–43*).

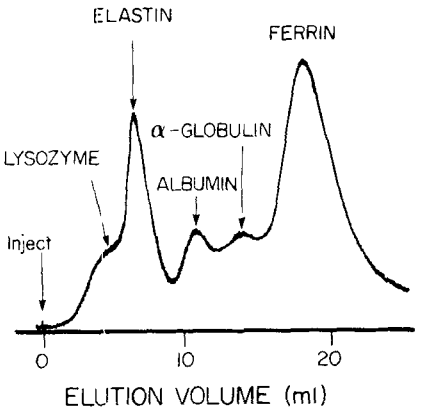

FIG. 7. Separation of proteins by flow FFF.

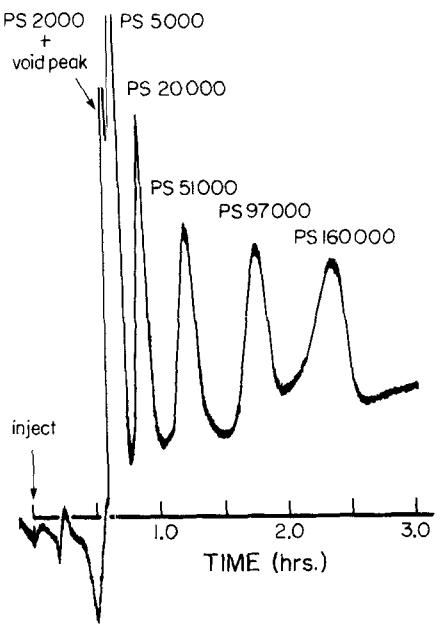

FIG. 8. Separation of linear polystyrene fractions of the indicated molecular weights by thermal FFF using a temperature drop of 60°C.

A fractogram of a mixture of narrow polystyrene fractions is shown in Fig. 8 (*43*). In addition to linear polystyrenes, thermal FFF has been shown applicable to polyethylene (*44*), polyisoprene, polytetrahydrofuran, polymethyl methacrylate (*45*) and, in unpublished work, branched chain polystyrenes.

Electrical FFF has been less widely applied than any of the other major four subtechniques. However, electrical FFF has been shown applicable to proteins (*46, 47*).

Steric FFF—which represents a different mode of operation (see Fig. 4) rather than a different subtechnique—has now been applied in our laboratory to the separation and characterization of a variety of larger particles (greater than 1 μm in diameter). Among the particles studies are red blood cells and various other cell types (*48*), residues from coal liquefaction (*49*), chromatographic support materials (*50*), large polystyrene latex beads (*51*), silica particles, and glass beads (*12*).

While the above examples illustrate the wide range of applicability of field-flow fractionation, these examples represent a bare beginning in the fractionation and characterization of complex high molecular weight materials. The difficulty in dealing with these complex materials using conventional fractionation techniques, coupled with the relatively high efficacy of FFF in this range, promises an ever-widening horizon for this promising and versatile technique.

Acknowledgment

This work was supported by Department of Energy Grant No. De-AC02-79EV10244.

REFERENCES

1. J. C. Giddings, *Sep. Sci., 1*, 123 (1966).
2. J. C. Giddings, *J. Chromatogr., 125*, 3 (1976).
3. J. C. Giddings, S. R. Fisher, and M. N. Myers, *Am. Lab., 10*, 15 (1978).
4. J. C. Giddings, M. N. Myers, K. D. Caldwell, and S. R. Fisher, in *Methods of Biochemical Analysis* (D. Glick, ed.), Wiley, New York, 1980, p. 79.
5. J. C. Giddings, *Anal. Chem., 53*, 1170A (1981).
6. J. C. Giddings, G. Karaiskakis, K. D. Caldwell, and M. N. Myers, *J. Colloid Interface Sci., 92*, 66 (1983).
7. J. J. Kirkland, C. H. Dilks, Jr., and W. W. Yau, *J. Chromatogr., 255*, 255 (1983).
8. J. J. Kirkland, S. W. Rementer, and W. W. Yau, *Anal. Chem., 53*, 1730 (1981).

9. J. C. Giddings, F. J. Yang, and M. N. Myers, *Sep. Sci., 12*, 381 (1977).
10. J. Gorse, T. C. Schunk, and M. F. Burke, *Sep. Sci. Technol.*, In Press.
11. J. C. Giddings and S. L. Brantley, *Ibid., 19*, 631 (1984).
12. J. C. Giddings and M. N. Myers, *Ibid., 13*, 637 (1978).
13. J. C. Giddings, *Ibid., 18*, 765 (1983).
14. J. C. Giddings, *Pure Appl. Chem., 51*, 1459 (1979).
15. J. C. Giddings, *J. Chem. Phys., 49*, 81 (1968).
16. M. E. Hovingh, G. H. Thompson, and J. C. Giddings, *Anal. Chem., 42*, 195 (1970).
17. J. C. Giddings, Y. H. Yoon, K. D. Caldwell, M. N. Myers, and M. E. Hovingh, *Sep. Sci., 10*, 447 (1975).
18. J. C. Giddings, *Sep. Sci. Technol., 13*, 241 (1978).
19. M. Martin and J. C. Giddings, *J. Phys. Chem., 85*, 72 (1981).
20. H. L. Lee and E. N. Lightfoot, *Sep. Sci., 11*, 417 (1976).
21. T. Takahashi and W. N. Gill, *Chem. Eng. Commun., 5*, 367 (1980).
22. F. J. F. Yang, M. N. Myers, and J. C. Giddings, *Anal. Chem., 46*, 1924 (1974).
23. J. F. Moeller, T. H. Dickinson, M. N. Myers, and M. Martin, *Ibid., 51*, 30 (1979).
24. F.-S. Yang, K. D. Caldwell, and J. C. Giddings, *J. Colloid Interface Sci., 92*, 81 (1983).
25. F.-S. Yang, K. D. Caldwell, M. N. Myers, and J. C. Giddings, *Ibid., 93,* 115 (1983).
26. M. N. Myers and J. C. Giddings, *Anal. Chem., 54*, 2284 (1982).
27. J. C. Giddings, *J. Chem. Educ., 50,* 667 (1973).
28. F.-S. Yang, K. D. Caldwell, J. C. Giddings, and L. Astle, *Anal. Biochem., 138*, 488 (1984).
29. K. D. Caldwell, T. T. Nguyen, J. C. Giddings, and H. M. Mazzone, *J. Virol. Methods, 1*, 241 (1980).
30. K. D. Caldwell, G. Karaiskakis, and J. C. Giddings, *J. Chromatogr., 215,* 323 (1981).
31. G. Karaiskakis, K. A. Graff, K. D. Caldwell, and J. C. Giddings, *Int. J. Environ. Anal. Chem., 12*, 1 (1982).
32. K. D. Caldwell, G. Karaiskakis, and J. C. Giddings, *Colloids Surf., 3,* 233 (1981).
33. K. D. Caldwell, G. Karaiskakis, M. N. Myers, and J. C. Giddings, *J. Pharm. Sci., 70*, 1350 (1981).
34. J. J. Kirkland and W. W. Yau, *Science, 218*, 121 (1982).
35. J. C. Giddings, F. J. Yang, and M. N. Myers, *Ibid., 193*, 1244 (1976).
36. J. C. Giddings, G. C. Lin, and M. N. Myers, *J. Colloid Interface Sci., 65*, 67 (1978).
37. J. C. Giddings, F. J. Yang, and M. N. Myers, *J. Virol., 21*, 131 (1977).
38. J. C. Giddings, F. J. Yang, and M. N. Myers, *Anal. Chem., 48*, 1126 (1976).
39. J. C. Giddings, G. C. Lin, and M. N. Myers, *J. Liq. Chromatogr., 1,* 1 (1978).
40. S. L. Brimhall, M. N. Myers, K. D. Caldwell, and J. C. Giddings, *J. Polym. Sci., Polym. Lett. Ed., 22,* 339 (1984).
41. J. C. Giddings, K. D. Caldwell, and M. N. Myers, *Macromolecules, 9*, 106 (1976).
42. J. C. Giddings, L. K. Smith, and M. N. Myers, *Anal. Chem., 47*, 2389 (1975).
43. J. C. Giddings, M. Martin, and M. N. Myers, *J. Polym. Sci., Polym. Chem. Ed., 19*, 815 (1981).
44. S. L. Brimhall, M. N. Myers, K. D. Caldwell, and J. C. Giddings, *Sep. Sci. Technol., 16*, 671 (1981).
45. J. C. Giddings, M. N. Myers, and J. Janca, *J. Chromatogr., 186*, 261 (1979).
46. L. F. Kesner, K. D. Caldwell, M. N. Myers, and J. C. Giddings, *Anal. Chem., 48*, 1834 (1976).
47. J. C. Giddings, G. C. Lin, and M. N. Myers, *Sep. Sci., 11,* 553 (1976).

48. K. D. Caldwell, Z.-Q. Cheng, P. Hradecky, and J. C. Giddings, *Cell Biophysics*, In Press.
49. H. Meng, K. D. Caldwell, and J. C. Giddings, *Fuel Processing Technol., 8,* 313 (1984).
50. J. C. Giddings, M. N. Myers, K. D. Caldwell, and J. W. Pav, *J. Chromatogr., 185*, 261 (1979).
51. R. E. Peterson, II, M. N. Myers, and J. C. Giddings, *Sep. Sci. Technol., 19*, 307 (1984).